Carbohydrate Polymers 88 (2012) 299–307

Contents lists available at SciVerse ScienceDirect

Carbohydrate Polymers

journal homepage: www.elsevier.com/locate/carbpol

# Processing and characterization of starch-based materials from pehuen seeds (*Araucaria araucana* (Mol) K. Koch)

J. Castaño[a,b], R. Bouza[c], S. Rodríguez-Llamazares[d,*], C. Carrasco[a,**], R.V.B. Vinicius[e]

[a] *Materials Engineering Department, Universidad de Concepción, Edmundo Larenas 270, Concepción, Chile*
[b] *Unidad de Desarrollo Tecnológico, Universidad de Concepción, Avda. Cordillera 2634, Coronel, Chile*
[c] *Departamento de Física, E.U.P. Ferrol, Universidad de A Coruña, Avda. 19 de Febrero s/n, 15405 Ferrol, Spain*
[d] *Research Center of Advanced Polymers (CIPA), Conicyt-Regional R08C1002, Avda. Cordillera 2634, Concepción, Chile*
[e] *Institute of Chemistry–Organic Chemistry Department, Universidade Federal do Rio Grande do Sul, Av. Bento Gonçalves, 9500 Agronomia, 91.501-970 Porto Alegre, RS, Brazil*

ARTICLE INFO

*Article history:*
Received 10 October 2011
Received in revised form
18 November 2011
Accepted 5 December 2011
Available online 17 December 2011

*Keywords:*
Thermoplastic starch
Pehuen starch
Glycerol
Sorbitol
Biodegradable

ABSTRACT

Starch isolated from pehuen seed (*Araucaria araucana* (Mol) K. Koch) was employed for producing thermoplastic starch (TPS). Pehuen starch was characterized, stating that the granules are rounded and small (12–21 μm), with an amylose content range 38–40%, a crystalline C-type structure and thermally stable, with decomposition temperature above 300 °C.

The effect of plasticizer type (glycerol and sorbitol) and starch/plasticizer ratio on TPS properties was also investigated. X-ray diffraction patterns of TPS showed the formation of processing-induced crystallinity, which depended on plasticizer employed. Thus, glycerol plasticized TPS presented the $V_H$-type structure, while sorbitol plasticized TPS presented the $E_H$-type structure. Sorbitol plasticized TPS had a higher thermal stability than glycerol plasticized TPS. Sorbitol plasticized TPS provided a material with more brittles and less flexibility. In contrast, glycerol plasticized TPS was tough and ductile. The tensile strength of TPS decreased with the increase in plasticizer content.



## 1. Introduction

In the past decade of growing environmental concerns, the use of starch-based resources in non-food applications has been developed, in response to the need for finding substitutes to petroleum-based plastics. In particular, granular starch produced by green plants has attractive characteristics such as natural availability, biodegradability, low cost and easy chemical and physical modifications that permit new applications (Guimarães, Wypych, Saul, Ramos, & Satyanarayana, 2010; Gross & Kalra, 2002; Martin, Averous, & Della Valle, 2003; Zullo & Iannace, 2009). Variations in size, shape, size distribution, degree of association and composition of starch granules reflect their botanical origin and growth conditions. These characteristics could have a profound influence on the final properties of starch-based plastic materials. Corn, potato and wheat starches are more often cited in scientific literature as raw materials for fillers in traditional plastics (Averous & Halley, 2009; Mani & Bhattacharya, 2001; Taguet, Huneault, & Favis, 2009), as well as in the development of biodegradable thermoplastic starch (Van Soest, Benes, & De Wit, 1996; Zullo & Iannace, 2009). An additional candidate for economic and efficient production and development of plastic materials is pehuen, the seed of *Araucaria araucana* (Mol) K. Koch conifer tree (common name Araucaria or Pehuen in the Mapuche language), which is endemic in temperate forests of Chile and Argentina (Aagesen, 2004; Herrmann, 2006). There are some 441,000 ha of *A. araucana* forest in the world, with 59% located in Chile.

Starch is the main component of the *A. araucana* seed (around 80%), and it can be isolated easily: a water treatment under mild conditions (without any additive) is commonly sufficient, in part due to the low content of phenolic compounds (Henríquez et al., 2008). The pehuen starch has low contents of ash, lipids, protein and crude fiber. Its granules are small and rounded (ca. 14 μm diameter), and their surface is smooth, with no evidence of erosion. The absence of surface irregularities such as channels and pores in corn-based granules is thought to affect their reactivity (when they are modified by chemical treatment) as well as some other physicochemical and functional properties (Bello-Pérez et al., 2006).In contrast to most synthetic polymers, starch is not truly thermoplastic. It occurs as partially crystalline, water-insoluble granules that may be destructurized in the presence of diluents (usually water), under pressure and at high temperatures, with or without shear stress. When dried, the resulting product is glassy at room temperature and its glass transition temperature is higher

* Corresponding author. Tel.: +56 41 2661216; fax: +56 41 2751233.
** Corresponding author. Tel: +56 41 2207170; fax: +56 41 2203391.
*E-mail addresses:* s.rodriguez@udt.cl (S. Rodríguez-Llamazares), ccarrascoc@udec.cl (C. Carrasco).

0144-8617/$ – see front matter © 2011 Elsevier Ltd. All rights reserved.
doi:10.1016/j.carbpol.2011.12.008

than its degradation temperature (Liu, Xie, Yu, Chen, & Li, 2009). Plasticizers are typically added to obtain so called *thermoplastic starch*, which is then amenable to processing by extrusion or molding.

Starch granule size is crucial for its processability as a thermoplastic material. Thus, for example, Chen, Schols, and Voragen (2004) found that the substitution degree increases when the granule size decreases, while Tang, Watanabe, and Mitsunaga (2002) demonstrated that smaller granules exhibited greater swelling degree and enzyme susceptibility. Furthermore, Franco, Ciacco, and Tavares (1998) reported that waxy corn starch granules with a small diameter hydrolyze easier than larger ones, while Daouda, Aboubakar, Dally, Pierre, and Kouame (2009) confirmed that smaller granules of cassava starch are more resistant to swell than the thickest ones.

Previous studies have shown that amylose/amylopectin ratios influence the structure, properties and processability of starch-based materials (Chaudhary, Torley, Halley, McCaffery, & Chaudhary, 2009; Thunwall, Boldizar, & Rigdahl, 2006; Van Soest, Benes, et al., 1996). Starches with higher amylose content produce polymers with superior strength and toughness (Almeida et al., 2010). Thus, for example, Yu and Christie (2005) found that both tensile modulus and yield stress of thermoplastic corn starch increased with the increasing amylose content of raw material. However, the processing of this high amylose starches is more difficult than that of normal starches, partly due to the higher die pressure and torque that are required because of the viscosity of these starches.

Hoover, Hughes, Chung, and Liu (2010) have described the effect of amylose content on starch properties, who defined the term *retrogradation* to describe crystallinity changes that occur upon cooling and storage of gelatinized starch. Earlier, Miles, Morris, Orford, and Ring (1985) had demonstrated that the amylopectin component is responsible for the thermally reversible crystallinity in a pea starch gel, although this does not rule out the co-precipitation and co-crystallization of amylose with amylopectin. Thus, retrogradation of corn starch was directly proportional to the number of short chains of amylopectins with degree of polymerization 16–30 and inversely proportional to those chains with degree of polymerization 6–11 (Shi & Seib, 1995). However, other authors (Matalanis, Campanella, & Hamaker, 2009) have reported that short-term changes in starch gel crystallinity are related to its amylose content, while long-term changes are clearly attributable to amylopectin retrogradation.

In addition to the properties of starch granules, plasticizers play an important role in the processability of starch-based materials. Glycerol and water in particular, but also polyols (xylitol, maltitol, sorbitol), urea and formamide, are some of the most commonly employed plasticizers (Adeodato, Altenhofen, Oliveira, & Masumi, 2011). Thus, for example, Bourtoom (2008) evaluated their role in affecting the mechanical properties of thermoplastic starch films; they found that sorbitol plasticized films had a more rigid structure than those plasticized with glycerol and poly(ethylene glycol). Indeed, low-molecular-weight polyols are more effective: short plasticizers penetrate more easily into the amylopectin gel balls and reduce the H-bonding between polymer chains.

Based on the summarized arguments, and following up on a published preliminary report (Bello-Pérez et al., 2006; Henríquez et al., 2008), it is anticipated that pehuen seeds should be excellent precursors for starch-based materials with adequate performance characteristics. Here, we report the results of morphological, structural and thermal characterization of pehuen starch granules and thermoplastic starch, and we describe the influence of plasticizer type and starch/plasticizer ratio on the thermal and mechanical properties of the final product.

## 2. Experimental

### 2.1. Materials

Starch was isolated from ripe pehuen seeds collected in the Chilean forest, using the isolation method proposed by Henríquez et al. (2008).

The plasticizers used were glycerol with a 99.5% purity (Winkler, USA) and sorbitol with moisture content of 30% (Reutter China).

### 2.2. Characterization of pehuen starch

The composition of native pehuen starch (i.e., moisture, ash, lipid, protein and total starch content) was determined according to standardized methods (see Table A1). Swelling capacity, water absorption capacity and solubility index were determined by using the procedures outlined by Sánchez and Aristizábal (2007).

The amylose content was determined by a colorimetric method (EN ISO 6647 parts I and II), which is based on amylose-iodine complex formation. The absorbance was measured at 620 nm by using an UV spectrophotometer (Perkin Elmer Lambda 35, Kyoto, Japan), and the amylopectin content was calculated by difference.

The particle size distribution was determined with a Beckman Coulter laser diffraction analyzer equipped with a LS 2000 sampling unit (Beckman Coulter, Brea CA, USA). Native starch granules were separated by using an automatic vibratory sieve shaker. Only particles that passed through a 45 μm sieve were used in this study. At least three measurements were made to obtain the average distribution curves.

To complete the starch characterization, thermal properties of pehuen starch were assessed by differential scanning calorimetry (DSC) and thermogravimetric analyses (TGA). Morphological features of starch granules were observed by using scanning electron microscopy (SEM), while their crystalline structure was determined by X-ray diffraction (XRD). Other measurement conditions are summarized in Section 2.4.

### 2.3. Preparation of thermoplastic starch (TPS)

Before melt-blending, pehuen starch and liquid plasticizers were premixed by hand at room temperature. A Haake internal mixer (Polysystem Rheocord, Waltham, USA) was used to prepare the TPS. The samples were blended at 120 °C with a rotor speed of 60 rpm for 15 min. The TPS compositions are shown in Table 1.

The TPS materials were injection-molded by using a Minijet II (Haake Thermo Scientific, Waltham, USA); the conditions of this process depended on the type of plasticizer used. Thus, in glycerol plasticized TPS, the processing temperature in the cylinder was 160 °C; its mold temperature, 50 °C, and its injection pressure, 350 bar. In sorbitol plasticized TPS, the temperature was 190 °C; its mold temperature, 100 °C, and its injection pressure, 550 bar.

### 2.4. Characterization of thermoplastic starch

#### 2.4.1. Scanning electron microscopy (SEM)

Starch granules and fracture surfaces of TPS were observed in a scanning electron microscope (JEOL-JSM 6380 LV, Tokyo, Japan). The molding specimens of TPS were cooled in liquid nitrogen before breaking. The fracture surfaces were coated with a gold film of ca. 50 nm and the images were taken at an accelerating potential of 20 kV.

#### 2.4.2. Thermal analysis: differential scanning calorimetry (DSC) and thermogravimetric analysis (TGA)

Crystallization experiments were carried out with a Perkin-Elmer DSC7-7700 differential scanning calorimeter (Waltham,

**Table 1**
TPS compositions and thermal properties.

| Sample | Glycerol (wt.%) | Sorbitol[a] (wt.%) | Pehuen starch (wt.%) | Decomposition temperature (°C) | | Decomposition temperature (°C) | | Decomposition enthalpy (J/g) |
|---|---|---|---|---|---|---|---|---|
| | | | | $T_{-5\%}$ | $T_{-50\%}$ | Onset ($T_o$) | Peak ($T_d$) | $\Delta H_d$ |
| APG37 | 30 | | 70 | 128 | 303 | 202 | 208 | 140 |
| APG46 | 40 | | 60 | 117 | 302 | 200 | 204 | 201 |
| APS37 | | 30 | 70 | 177 | 312 | 202 | 207 | 106 |
| APS46 | | 40 | 60 | 168 | 310 | 200 | 206 | 126 |

[a] The sorbitol used was a technical grade at 70% purity and a moisture content of 30 wt.%.

USA), calibrated with indium ($T_m$ = 156.6 °C, $\Delta H_m$ = 28.45 kJ kg$^{-1}$) and zinc ($T_m$ = 419.47 °C, $\Delta H_m$ = 108.37 kJ kg$^{-1}$). Aluminum pans were used with sample weights of approximately 10 mg. DSC scans were made under an inert atmosphere with a nitrogen flow of 25 mL/min. DSC scans of both pehuen starch and TPS ranged between 30 and 210 °C. Decomposition onset temperature ($T_o$) and decomposition temperature ($T_d$) as well as decomposition enthalpy of ($\Delta H_d$) were obtained from DSC scans of TPS.

Thermal stability was evaluated with a NETZSCH 209 F3 (model Tarsus apparatus, Selb, Germany). TGA scans were recorded at 10 °C/min, in a range between 30 and 900 °C, under nitrogen atmosphere (20 mL/min).

*2.4.3. X-ray diffraction (XRD)*

The crystalline structure of pehuen starch and TPS was analyzed at room temperature by means of XRD, using a Bruker Endeavor diffractometer (Model D4/MAX-B, Karlsruhe, Germany), operating at 40 kV, 20 mA and Cu-Kα radiation (1.541 Å). The scans were obtained in the reflection mode over a 2$\theta$ range 4–35°, in steps of 0.02°, at 0.008°/min. Peak fitting analysis was also made using a Gaussian distribution function.

The results were quantified by using the following equation (Wang et al., 2006):%Crystallinity = $\frac{A_c}{A_c+A_a} \times 100$Here, $A_c$ and $A_a$ refer to the crystalline and amorphous areas in the diffractogram, respectively. The contribution of the amorphous part was analyzed in the range among $4° \leq 2\theta \leq 35°$; the procedure used was that of Frost, Kaminski, Kirwan, Lascaris, and Shanks (2009). Baseline correction was followed by noise reduction, using a 50-point Savitzky–Golay moving filter. Iterative smoothing was performed by using Matlab (version 7.4) with PLS toolbox (version 4.0.2); in the case of two consecutive iterated curves, the lower of the two intensities for the same 2$\theta$ value was taking as condition (Brückner, 2000).

*2.4.4. Tensile properties*

Tensile properties were evaluated in a universal testing machine (Emic DL 2000, Paraná, Brazil), according to ASTM D-638 standard using specimen bar type V. Before measurement, all test samples were conditioned for 48 h at 23 °C, with 50% of relative humidity in agreement with ASTM D-618. The crosshead speed was set at 1.0 mm/min. Values reported (strength and elongation at break) were averages of at least five specimens.

## 3. Results and discussion

*3.1. Characterization of pehuen starch*

Two different polysaccharides are present in starch: the linear (1,4)-linked α-D-glucan amylose and the highly (1,6)-branched α-D-glucan amylopectin, both represent approximately 98–99% of the dry weight. These polysaccharides have different properties and are not suitable for the same applications (Zobel, 1988). The ratio of these two polysaccharides varies according to the botanical source. The "waxy" starches contain less than 5% amylose, "normal" ranging between 20% and 30% and "high" amylose starches greater than 40% (Almeida et al., 2010).

The composition of pehuen starch (see Table A1) was in agreement with values reported by Henríquez et al. (2008). The amylose and amylopectin content obtained by colorimetric method were 38–40% and 60–62%, respectively. Hence, the pehuen starch could be considered as a high amylose starch. The amylose content was higher than that reported for other starch sources, such as corn (23.4–24.5%), potato (18.0–25.4%), cassava (17.9–18.6%) and rice (13.2%) (Srichuwong, Sunarti, Mishima, Isono, & Hisamatsu, 2005; Takizawa Da Silva, Konkel, & Demiate, 2004).

SEM micrographs and size distribution of the pehuen starch granules are shown in Fig. 1. The granule surface is smooth, with

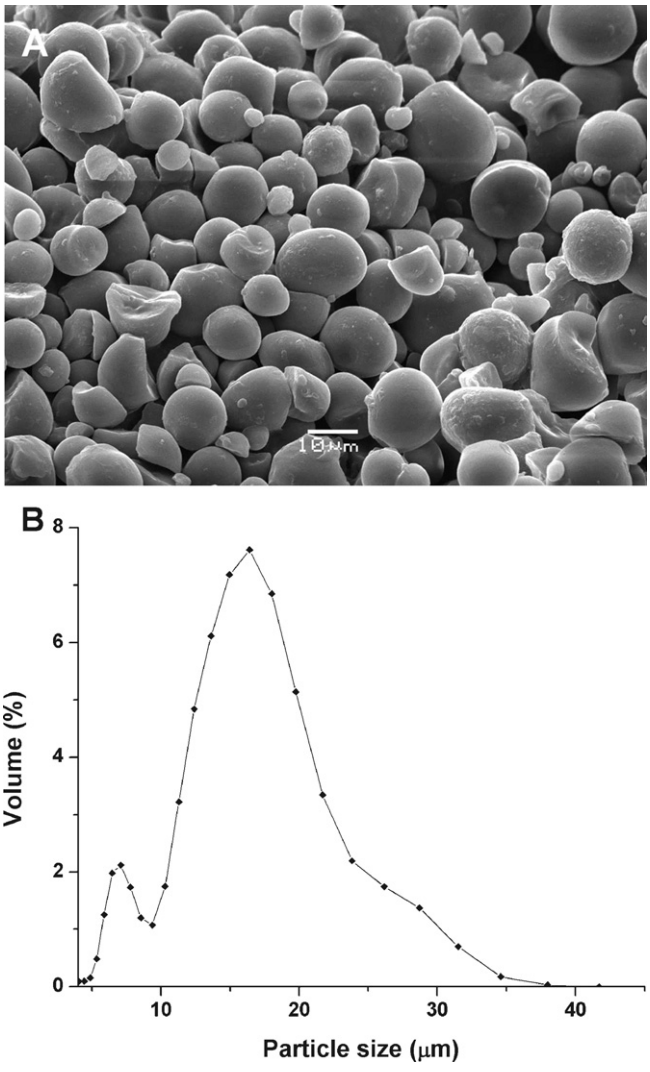


**Fig. 1.** (A) SEM micrograph and (B) particle-size distribution of pehuen starch.

no irregularities or erosion; besides, most of them showed a flat surface on one side (Fig. 1A); as mentioned in Section 1 this characteristic can favor starch reactivity and its physicochemical and functional properties (Bello-Pérez et al., 2006; Tharanathan, 2005). The diameter of granule measured in SEM micrographs ranged between 4 and 18 μm (for 500 starch granules), which is consistent to particle size distribution obtained by laser granulometry. A typical bimodal size distribution can be observed in Fig. 1B. Peaks presented a narrow size distribution: the lower intensity peak corresponded to smaller-sized granules (6–8 μm), and the higher one to large-sized granules (12–21 μm). These large-sized granules represent the large fraction of pehuen granules.

When amylose content and granule morphology of *A. araucana* and *A. angustifolia* are compared (same genus (*Araucaria juss*) and Syn. sect. *Columbea*), it is possible to observe that starch granules of *A. angustifolia* have lower amylose content (around 25%, Bello-Pérez et al., 2006) than that of pehuen starch. Starch granules of *A. angustifolia* reported by Bello-Pérez et al. (2006) are a mixture of rounded and oval granules, with size between 10 and 25 μm. Starch granules of *A. araucana* have some differences in morphology and lower granule size. Wang et al. (2006) reported that small granules of different Chinese yam (from the same species, *Dioscorea opposita* Thunb.) have higher amylose content than the bigger ones, which could explain the differences in amylose content found between the *Araucaria* species. However, Thys et al. (2008) reported starch granules of *Araucaria angustifolia* similar in shape and size to the starch granules of *A. araucana* reported in this work, but with an amylose content of 25%. Therefore, it is possible to infer that amylose content of starch granules in *Araucaria* sp. is directly related with botanical species. It is not possible to disregard that the variation in amylose content of starches could also be attributed to the different cultivar zone, starch isolation procedures and analytical methods used to determine amylose content (Singh, Singh, Kaur, Singh Sodhi, & Singh Gill, 2003; Tester, Karkalas, & Qi, 2004).

XRD diffractogram of pehuen starch is showed in Fig. 2A. The diffraction pattern corroborated the C-type structure of pehuen starch, with very strong reflection at 2$\theta$ values of 16.9° and 22.8° (see Table A2). C-type pattern of pehuen starch showed diffraction peaks corresponding to both A-type and B-type patterns. The peak at 2$\theta$ value of 5.5° is characteristic of B-type pattern, while 22.7° is indicative of A-type pattern. Similar results were reported by Cheetham and Tao (1998), who studied the variation in crystalline type with amylose content in maize starch granules. They found that the transition of crystalline type from A through C to B occurred at approximately 40% of amylose content, as could be the case for pehuen starch.

It can also be observed in Fig. 2A that underlying background scatter reflects a low crystallinity level of pehuen starch. The determination of amorphous scattering region is a critical step of crystallinity measurements for semi-crystalline polymers such as starch. Many arbitrary methods have been developed for this purpose, each of them with varying conditions and success. We decide to use an uncomplicated, quick and objective method reported by Frost et al. (2009). In the smoothing algorithms for amorphous background estimation, the following parameters were taken into account: polynomial order, number of iteration and point of window. The degree of crystallinity of pehuen starch was calculated from the relative areas of crystalline and amorphous regions. The value obtained was 15.1%, which is in the range of values reported for starches with 40–50% of amylose content (Mani & Bhattacharya, 2001). It is well known that the degree of crystallinity in starch granules is inversely proportional to the amylose content (Frost et al., 2009; Kubo et al., 2008; Mani & Bhattacharya, 2001). According to some studies on C-type polymorphism, amorphous regions are mainly located in the center of starch granules, while crystalline areas mainly existed in the exterior of granules (Pérez & Bertoft, 2010; Tester et al., 2004).

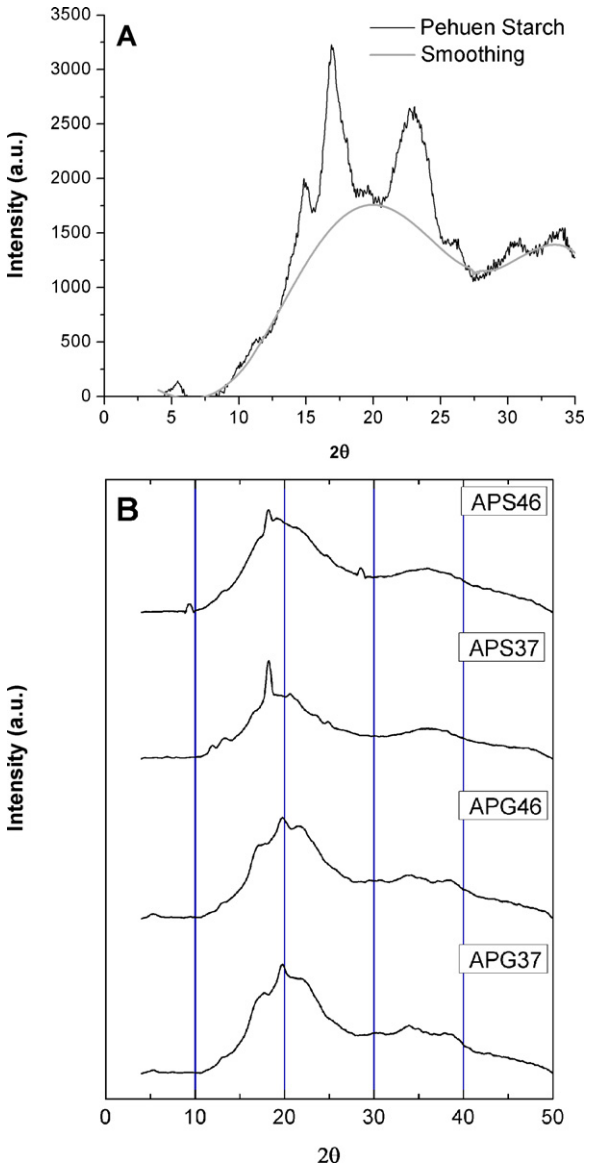


**Fig. 2.** X-ray diffraction pattern of: (A) pehuen starch and (B) studied TPS.

Thermal stability of pehuen starch was analyzed by TGA. The weight loss during heating of pehuen starch occurred in two mass-loss steps (Fig. 3). The first step corresponded to the evaporation/dehydration process, which began immediately after the temperature increased and finished at around 130 °C. The percentage of weight loss in this step was 8.1%, which is related to moisture content of the pehuen starch. The second mass-loss step corresponded to the thermal decomposition process that started around 300 °C. The mass-loss of 71.7% calculated from a range between 302 and 602 °C is related to the exothermic peak centered at 321 °C (Fig. 3: DTG). The second thermal decomposition is due to burning organic matter. The weight loss observed in this temperature range has been assigned to intermolecular dehydration to form leavoglucosan and some volatile products, such as carbon dioxide, lower aldehydes, methylfuranes, and ketones (Chandra & Rustgi, 1997; Xia, Wenyuan, Qianqian, Luqi, & Changxiao, 2011). The residue mass at 900 °C was negligible.

DSC scan of pehuen starch displayed a broad peak around 120 °C, which does not correspond to their melting temperature. The low

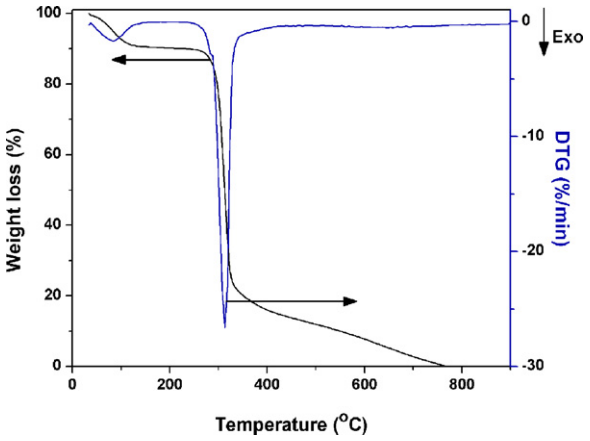


**Fig. 3.** TGA and DTG of pehuen starch.

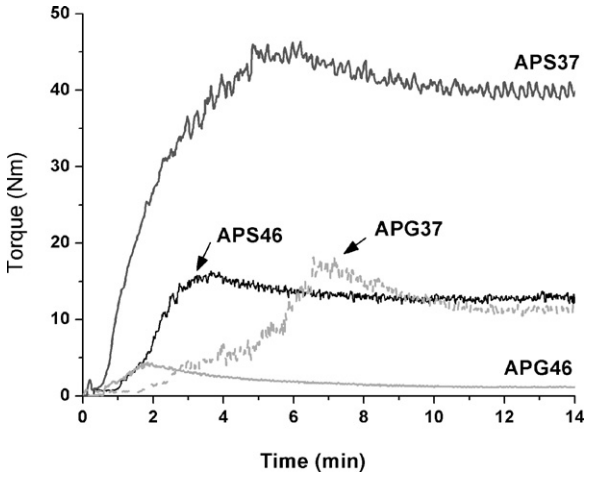


**Fig. 4.** Torque variation as a function of time for TPS samples.

water content (less than 30%, w/w) in starch made experimentally inaccessible the determination of melting temperature, due to thermal degradation of starch occurred before it melted (Parker & Ring, 2001). It is accepted that starch melting is a solvent-facilitated process. It is postulated that water permits the swelling/hydration of amorphous parts of starch granules. The crystallites that couple with the swelling/hydration amorphous part melts co-operatively, which is called co-operative first-order transitions (Biliaderis, Page, Maurice, & Juliano, 1986; Wang, Bogracheva, & Hedley, 1998). In the absence of water, the endothermic peak can be attributed to small order/disorder transitions. These transitions are due to loss of structural water of starch granules, fact that can be deduced from the temperature range where water loss occurs during heating (Fig. 3: TGA). This thermal transition is also represented by endothermic peak in the DSC scan.

### 3.2. Characterization of TPS

#### 3.2.1. Processing property

Starches are non-plastic due to the intra and inter molecular hydrogen bonds between the hydroxyl groups of their principal components (Liu et al., 2009). Thermoplasticization process of starch involves the partial or complete destruction of the initial crystalline order. In the presence of suitable plasticizers, mechanical shear stresses and heat, the molecular chains of starch gain mobility and the hydrogen bonding interactions with the plasticizer are favored (Zullo & Iannace, 2009). Tan, Wee, Sopade, and Halley (2004) found that the properties of plasticizer that mainly affect gelatinization of starch are viscosity, diffusivity and molecular. In this way, water is undoubtedly the most suitable plasticizer for starch because it is a small molecule that can easily penetrate in the starch structure breaking amylopectin and amylose bonds. However, water plasticized starch are fragile materials due to water evaporation. On the other hand, it is well known that to plasticize dry starch a high quantity of plasticizer is required, reason why TPS are commonly prepared using polyols with diverse quantities of water.

Two different polyols, glycerol and sorbitol, and different proportions of each ones were employed to prepare TPS materials (Table 1). The Haake torque rheometer provides a convenient tool to study the rheological properties and starch processing, in particular for the system with lower moisture content. The variation torque as a function of time for studied TPS is illustrated in Fig. 4. All TPS showed a similar tendency in the change of torque with time, increasing rapidly to maximum and then reaching a plateau that decreased gradually. Equilibrium torque is related to the viscosity of the plasticized starch during melting processing, and its viscosity at once is related to the mobility of the starch molecular chains under shear forces and temperature. Thus, higher plasticizer content (40 wt.%) made a significant change on the viscosity of TPS. In the plateau the reduction of torque was 25 and 65% for glycerol and sorbitol plasticized TPS, respectively. The plasticizer molecules interact through hydrogen bond with macromolecules of starch, allowing more mobility of macromolecules chains. Additionally, the energy necessary for plasticizing the TPS is lower when glycerol is used as a plasticizer. It is important to note that the torque curves of sorbitol plasticized TPS were less stable, and that the time to reach the plateau was higher than that of glycerol plasticized TPS. Pushpadass et al. (2009) found that at lower moisture content, the fragmentation of amylopectin chains in starch decreased, increasing thence amyloce content. This fact could explain the higher torque required to plasticize pehuen starch using liquid sorbitol.

#### 3.2.2. Scanning electron microscopy

SEM micrographs of the fractured surfaces of TPS showed the absence of starch granules, which is an evidence of plasticization of pehuen starch under the used processing conditions (Fig. 5). The surface morphology depended fundamentally on type of plasticizer. Thus, a continuous phase was observed in glycerol plasticized TPS, as well as a rough and homogeneous surface. Zhou, Cui, Jia, and Xie (2009) reported that the rough surface could be a suggestion of a semicrystalline material.

The surfaces of TPS plasticized with sorbitol were smooth with a large amount of voids, indicating the evaporation of extra water and/or a partial miscibility between this plasticizer and pehuen starch. The voids were circular and uniformly distributed in the fractured surface; the size of the voids was smaller in TPS with higher sorbitol content (Fig. 5C and D). It is important to note that sorbitol plasticized TPS were spontaneously fractured when submerged in liquid nitrogen, showing high brittleness, demonstrating that the evaporation of extra water occurred.

The fragility of sorbitol plasticized TPS can be attributed to the higher molecular weight of sorbitol in comparison to glycerol. Plasticizer molecules with lower sizes penetrate more easily into the amylopectin chains forming amylopectin gel-ball, an essential step to make the plasticization of starch.

#### 3.2.3. Thermal properties

The thermal stability of TPS was assessed by thermogravimetric analysis. The temperature at which the 5% and 50% of weight loss occurs, $T_{-5\%}$ and $T_{-50\%}$, respectively, are listed in Table 1. TGA curves of the TPS showed a similar tendency; however, it was observed that the type and concentration of plasticizer had influenced on

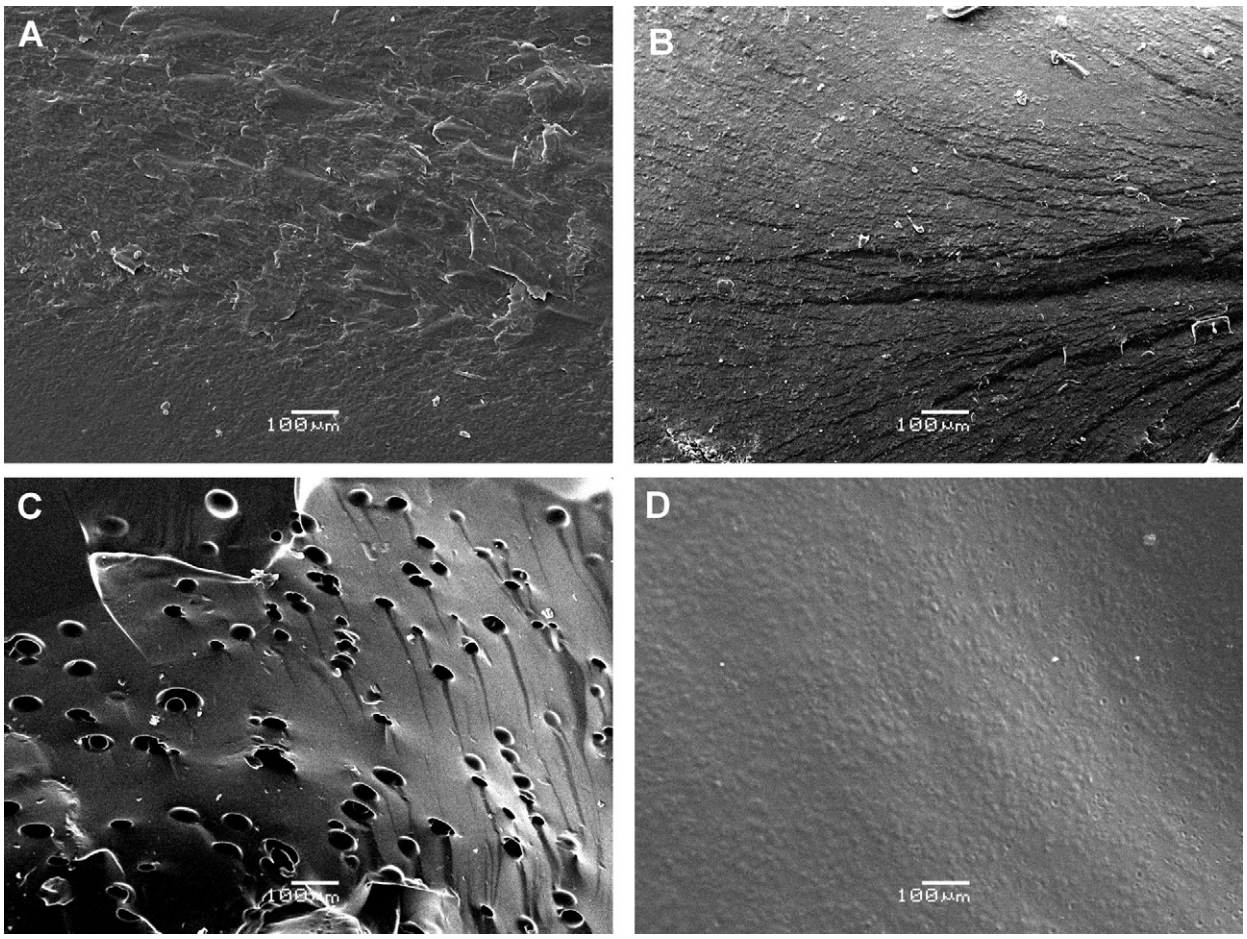


**Fig. 5.** SEM micrographs of fracture surfaces of molded TPS specimens, using (A) 30 wt.% of glycerol; (B) 40 wt.% of glycerol; (C) 30 wt.% of sorbitol and (D) 40 wt.% of sorbitol.

the thermal stability of TPS. By increasing the plasticizer content in 10 wt.%, the $T_{-5\%}$ decreased around 10 °C. Sorbitol plasticized TPS had a higher thermal stability than glycerol plasticized TPS, which could be attributed to the high molecular weight of sorbitol (Qiao, Tang, & Sun, 2011).

Thermal properties obtained from DSC thermograms of TPS are also presented in Table 1. DSC curves of every TPS showed a broad endothermic peak at around 205 °C, corresponding to decomposition temperature. We notice that this transition is concomitant with a mass loss observed by means of TGA (Leblanc et al., 2008). The peak of the decomposition temperature became broader with increasing plasticizer content. The decomposition enthalpy of glycerol plasticized TPS was higher than that of sorbitol plasticized TPS. The heat difference involved in the decomposition transition is attributed to the increase of the amylopectin/plasticizer interactions.

### 3.2.4. X-ray diffraction

X-ray diffraction patterns of TPS are presented in Fig. 2B. The thermoplasticization processes lead to disruption of starch structure and, as a result the reduction of crystallinity of thermoplastic starch is reached. Two types of crystallinity are reported in TPS after processing by kneading, extrusion, compression molding or injection molding: residual crystallinity and processing-induced crystallinity (Raquez et al., 2008; Van Soest, Hulleman, De Wit, & Vliegenthart, 1996). The first one is associated to native A-, B-, or C-type remainder crystallinity and is due to incomplete melting of the starch native crystal. The processing-induced crystallinity is also known as V-type crystallinity and it is attributed to crystal structure of single left-handed helix of amylose (Nishiyama et al., 2010) with a complexing agent found inside the helix channel, which are both formed during thermo-mechanical processing. Three V-type crystal structures of the single-helical amylose, $V_H$, $V_A$ and $E_H$ type have been reported for TPS materials (Dai, Chang, Yu, Ma, & Zhou, 2010; Radley, 1976).

Residual C-type crystallinity is not observed in thermoplastic pehuen starches, since there were not characteristic peaks in X-ray diffraction patterns (Fig. 2B). This indicates that the energy input in the torque rheometer was sufficient to plasticize the pehuen starch completely. However, the processing-induced crystallinity caused by the recrystallization of amylose complex with plasticizer (complexing agent) into single-helical structures was formed. The diffraction pattern of glycerol plasticized TPS can be assigned to the $V_H$ type structure (peak at around 20°), while sorbitol plasticized TPS, to the $E_H$ type structure (peak at around 17°) (Van Soest, Hulleman, et al., 1996). It is known that the $E_H$-type structure, stable at low moisture content, is transformed into a $V_H$-type structure by increasing water content (complexing agent) in the sample (Shogren, Fanta, & Felker, 2006; Van Soest, Hulleman, et al., 1996). In our case, the transformation of one structure to another is related to plasticizer type. The crystals of amylose complexed with glycerol ($V_H$-type) exhibit a packing of six-fold single helices (Buléon, Véronèse, & Putaux, 2007), while the crystals of amylose complexed with sorbitol ($E_H$-type), a guest molecule with larger size than glycerol, exhibit a packing of seven-fold single helices. Glycerol plasticized TPS presents a higher amount of molecules of complexing agent (glycerol) available to interact with amylose chains; therefore, $V_H$-type structure will be favored in these thermoplastic materials.

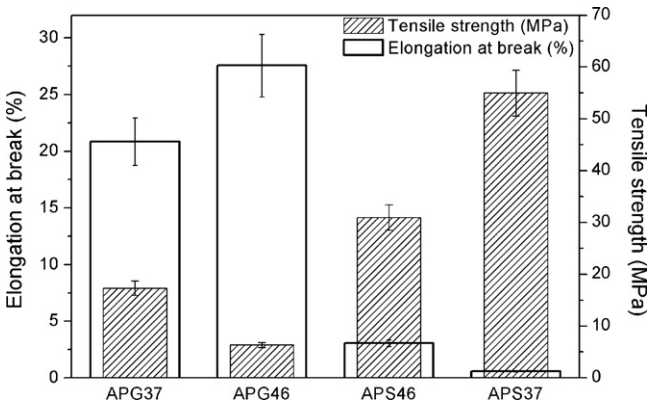


**Fig. 6.** Mechanical properties from traction test of TPS samples.

The percentage of processing-induced crystallinity of TPS was calculated from XRD data. Polynomial degree, number of iteration and point of windows values were kept constant for all diffractograms, in order to have the same relative error when comparing different samples. The calculated processing-induced crystallinity of TPS ranged from 4.7% to 6.4%. A constant 5.5% of crystallinity was determined for glycerol plasticized TPS, while for sorbitol plasticized TPS, crystallinity varied in function of plasticizer content, being 6.4% and 4.7% for samples APS37 and APS46, respectively. The high percentage of crystallinity obtained from sample APS37 could be related to a higher applied shear stress required to plasticize (Fig. 4); the orientation of amylose complex could be favored.

### 3.2.5. Tensile properties

The effect of type and content of plasticizer on the mechanical properties of thermoplastic starches is shown in Fig. 6. The plasticizer content has a similar effect independent of the plasticizer type: tensile strength decreased with the increase of plasticizer content, while the elongation at break also increased. Note the high values of elongation to break obtained for samples with 40 wt.% of plasticizer.

The mechanical properties of TPS, such as Young's Modulus, tensile strength and elongation at break, are affected by starch type. Chaudhary et al. (2009) reported that thermoplastic starch material obtained from waxy corn starch was a stiffer material, with a lower elongation at break; while that obtained from high amylose starch (50 and 80%) tended to be tougher than low amylose (28%). A comparison of the tensile strength of TPS from pehuen starch plasticized with 30 wt.% glycerol (about 8.0 MPa), with data found in literature for TPS with the same starch/plasticizer ratio (Zullo & Iannace, 2009), showed that measured values are comparable with TPS from starches with 80% of amylose content. As the pehuen starch has only 40% of amylose, the similitude in tensile strength could be attributed to several factors. Firstly, the number and length of branched chains of amylopectin and the molecular weight of amylose of pehuen starch could facilitate the entanglements of amylose and branched amylopectin chains. The entangled chains limit molecular movements thus increasing its strength. Secondly, the enhancement of mechanical properties could also be attributed to the formation of $V_H$ crystal polymorph (Chaudhary et al., 2009; Dai et al., 2010; Thunwall et al., 2006).The TPS prepared with sorbitol presented a characteristic of stiff materials, with high tensile strength and low elongation at break. This behavior could be associated to porosity found in the fractured surface of TPS. Furthermore, the original water in raw starch diffuses easily to surrounding amylose and amylopectin chains, facilitating starch to water–hydrogen bonds during extrusion (thermo-mechanical) process. The water present in sorbitol is not completely free to interact with the amylopectin and amylose chains, and on this account it is easily evaporated, producing the fragility of the TPS.

## 4. Conclusions

Starch isolated from pehuen seeds of *A. araucana* (Mol) K. Koch was characterized physicochemical, morphological, structural and thermally. The main characteristics observed were: (a) amylose content ranging between 38 and 40%, (b) small rounded starch granules (12–21 μm), (c) crystalline structure of a typical C-type pattern and (d) thermally stable, with decomposition temperature above 300 °C.

The effect of type and content of plasticizer on thermoplastic pehuen starch properties was also studied showing the potential of this starch as an excellent precursor for starch-based materials. No retained crystallinity was observed in studied TPS, while processing-induced crystallinity depends on plasticizer employed: glycerol plasticized TPS presented $V_H$-type structure, while sorbitol plasticized TPS presented the $E_H$-type structure. Thermal analysis studies showed that the type and concentration of plasticizer had influence on the thermal stability of TPS. Sorbitol plasticized TPS was more stable, since sorbitol has a higher thermal stability than glycerol. According to tensile properties, sorbitol plasticized pehuen starch provided a material with more brittleness and less flexibility. In contrast, glycerol plasticized pehuen starch made it more resistant and ductile. The enhancement of glycerol-plasticized pehuen starch mechanical properties could be attributed to both the nature of plasticizer and the formation of the $V_H$ crystal polymorph. In all TPS samples, the tensile strength decreased with the increase in plasticizer content, while the elongation at break increased.

## Acknowledgements

This work has been partially financed by CONICYT-REGIONAL R08C1002, Projects Fondef D08I1191 and D09I1195. Ms. Susana Castillo helped in samples preparations and testing.

## Appendix A.

See Tables A1 and A2 and Fig. A1.

**Table A1**
Moisture, proximate analysis and hydration properties of isolated pehuen starch.

| | Value | Reference testing |
|---|---|---|
| Moisture (%) | 7.1 ± 0.4 | Chilean Standard 176/1 of 84 |
| Ash (g/100 g dry starch) | 0.120 ± 0.005 | ASTM D1102-56 |
| Lipid (g/100 g dry starch) | 0.02 ± 0.13 | AOAC[a] 2003 |
| Protein (g/100 g dry starch) | 1.4 ± 0.4 | Kjendhal, AOAC 1990 |
| Total starch (g/100 g dry starch) | 84.00 ± 0.01 | AOAC 996.11 |
| Amylose (g/100 g dry starch) | 39 ± 2 | UNE-EN ISO 6647-1, UNE-EN ISO 6647-2 |
| Swelling capacity (mL water/g dry starch) | 2.0 ± 0.2 | Sánchez and Aristizábal (2007): ISSN 1020-4334 |
| Water retention capacity (g water/g dry starch) | 2.0 ± 0.2 | |
| Solubility index (g water/g dry starch) | 0.3 ± 0.2 | |

[a] AOAC, Association of Official Analytical Chemists.

**Table A2**
Crystallographic parameters of pehuen starch and reported A-type and B-type semicrystalline starches (Frost et al., 2009).

| Pehuen starch | | A-type (literature) | | B-type (literature) | |
|---|---|---|---|---|---|
| $2\theta$ (°) | Intensity | $2\theta$ (°) {$hkl$} | Intensity | $2\theta$ (°) {$hkl$} | Intensity |
| 5.5 | m | | | 5.5{001} | m |
| | | | | 10.8 {111} | m |
| 14.9 | vs | 14.8{140} | s | 14.8{140} | s |
| | | 16.6{131} | vs | | |
| 16.9 | vs | | | 17.0{131} | vs |
| | | 17.7{131} | s | | |
| 19.6 | m | | | 19.3{103} | s |
| | | | | 22.1{113} | vs |
| 22.8 | vs | 22.6{132} | vs | | |
| | | | | 23.8{132} | s |
| 26.1 | m | 26.3{142} | w | 26.1{142} | w |
| | | 30.1 | m | | |
| 31 | m | | | 30.9 | w |
| | | 33.2 | w | | |
| 34 | m | | | 34 | m |

s, strong; w, weak; m, medium; vs, very strong.

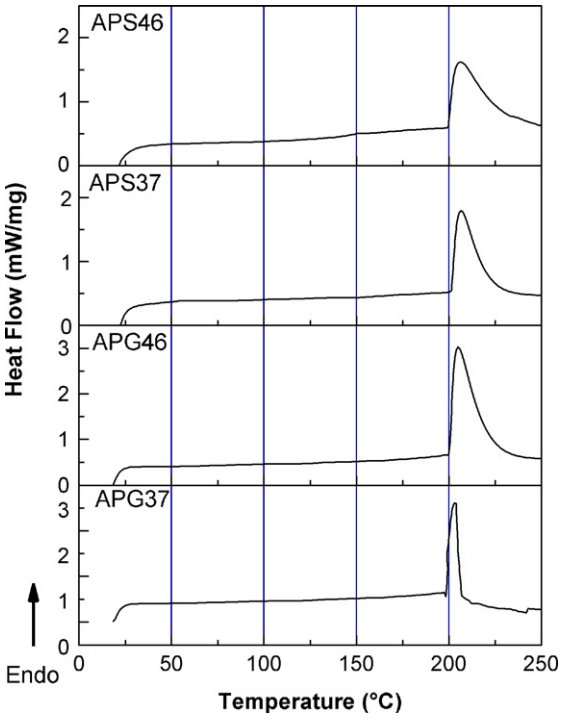


**Fig. A1.** DSC thermograms of thermoplastic starch with (APG37) 30 wt.% of glycerol, (APG46) 40 wt.% of glycerol, (APS37) 30 wt.% of sorbitol and (APS46) 40 wt.% of sorbitol.

## References


Aagesen, D. (2004). Burning monkey-puzzle: Native fire ecology and forest management in northern Patagonia. *Agriculture and Human Values*, *21*, 233–242.

Adeodato, M., Altenhofen, M., Oliveira, L., & Masumi, M. (2011). Natural-based plasticizers and biopolymer films: A review. *European Polymer Journal*, *47*, 254–263.

Almeida, M. R., Alves, R. S., Nascimbem, L., Stephani, R., Poppi, R. J., & De Oliveira, L. F. (2010). Determination of amylose content in starch using Raman spectroscopy and multivariate calibration analysis. *Analytical and Bioanalytical Chemistry*, *397*, 2693–2701.

Averous, L., & Halley, P. (2009). Review biocomposites based on plasticized starch. *Biofuels, Bioproducts & Biorefining*, *3*, 329–343.

Bello-Pérez, L., García-Suarez, F., Mendez-Montealvo, G., Oliveira, J., Lajolo, F., & Cordenunsi, B. (2006). Isolation and characterization of starch from seeds of *Araucaria brasiliensis*: A novel starch for application in food industry. *Starch/Stärke*, *58*, 283–291.

Biliaderis, C. G., Page, C. M., Maurice, T. J., & Juliano, B. O. (1986). Thermal characterization of rice starches: A polymeric approach to phase transitions of granular starch. *Journal of Agricultural and Food Chemistry*, *34*, 6–14.

Bourtoom, T. (2008). Plasticizer effect on the properties of biodegradable blend film from rice starch-chitosan. *Songklanakarin Journal of Science and Technology*, *30*, 149–165.

Brückner, S. (2000). Estimation of the background in powder diffraction patterns through a robust smoothing procedure. *Journal of Applied Crystallography*, *33*, 977–979.

Buléon, A., Véronèse, G., & Putaux, J. L. (2007). Self-association and crystallization of amylose. *Australian Journal of Chemistry*, *60*, 706–718.

Chandra, R., & Rustgi, R. (1997). Biodegradation of maleated linear low-density polyethylene and starch blends. *Polymer Degradation and Stability*, *56*, 185–202.

Chaudhary, A. L., Torley, P. J., Halley, P. J., McCaffery, N., & Chaudhary, D. S. (2009). Amylose content and chemical modification effects on thermoplastic starch from maize—Processing and characterisation using conventional polymer equipment. *Carbohydrate Polymers*, *78*, 917–925.

Cheetham, N. W. H., & Tao, L. (1998). Variation in crystalline type with amylose content in maize starch granules: An X-ray powder diffraction study. *Carbohydrate Polymers*, *36*, 277–284.

Chen, Z. H., Schols, H. A., & Voragen, A. G. J. (2004). Differently sized granules from acetylated potato and sweet potato starches differ in the acetyl substitution pattern of their amylose populations. *Carbohydrate Polymers*, *56*, 219–226.

Dai, H., Chang, P. R., Yu, J., Ma, X., & Zhou, P. (2010). Preparation and properties of thermoplastic pea starch using N,N-bis(2-hydroxyethyl)formamide as the plasticizer. *Polymer Engineering and Science*, *50*, 970–977.

Daouda, S., Aboubakar, S., Dally, L. I., Pierre, E., & Kouame, O. C. (2009). Thermal effects on granules and direct determination of swelling capacity of starch from a cassava cultivar (Attiéké Mossi 1) cultivated in Côte D'Ivoire. *African Journal of Biotechnology*, *8*, 3615–3622.

Franco, C. M. L., Ciacco, C. F., & Tavares, D. Q. (1998). The structure of waxy corn starch: Effect of granule size. *Starch/Stärke*, *50*, 193–198.

Frost, K., Kaminski, D., Kirwan, G., Lascaris, E., & Shanks, R. (2009). Crystallinity and structure of starch using wide angle X-ray scattering. *Carbohydrate Polymers*, *78*, 543–548.

Guimarães, J. L., Wypych, F., Saul, C. K., Ramos, L. P., & Satyanarayana, K. G. (2010). Studies of the processing and characterization of corn starch and its composites with banana and sugarcane fibers from Brazil. *Carbohydrate Polymers*, *80*, 130–138.

Gross, R. A., & Kalra, B. (2002). Biodegradable polymers for the environment. *Science*, *297*, 803–807.

Henríquez, C., Escobar, B., Figuerola, F., Chiffelle, I., Speisky, H., & Estévez, A. M. (2008). Characterization of piñon seed (*Araucaria araucana* (Mol) K. Koch) and the isolated starch from the seed. *Food Chemistry*, *107*, 592–601.

Herrmann, T. M. (2006). Indigenous knowledge and management of *Araucaria araucana* forest in the Chilean Andes: Implications for native forest conservation. *Biodiversity and Conservation*, *15*, 647–662.

Hoover, R., Hughes, T., Chung, H. J., & Liu, Q. (2010). Composition, molecular structure, properties, and modification of pulse starches: A review. *Food Research International*, *43*, 399–413.

Kubo, A., Yuguchi, Y., Takemasa, M., Suzuki, S., Satoh, H., & Kitamura, S. (2008). The use of micro-beam X-ray diffraction for the characterization of starch crystal structure in rice mutant kernels of waxy, amylose extender, and sugary. *Journal of Cereal Science*, *48*, 92–97.

Leblanc, N., Saiah, R., Beucher, E., Gattin, R., Castandet, M., & Saiter, J. M. (2008). Structural investigation and thermal stability of new extruded wheat flour based polymeric materials. *Carbohydrate Polymers*, *73*, 548–557.

Liu, H., Xie, F., Yu, L., Chen, L., & Li, L. (2009). Thermal processing of starch-based polymers. *Progress in Polymer Science*, *34*, 1348–1368.

Mani, R., & Bhattacharya, M. (2001). Properties of injection moulded blends of starch and modified biodegradable polyesters. *European Polymer Journal*, *37*, 515–526.

Martin, O., Averous, L., & Della Valle, G. (2003). In-line determination of plasticized wheat starch viscoelastic behavior: Impact of processing. *Carbohydrate Polymers*, *53*, 169–182.

Matalanis, A. M., Campanella, O. H., & Hamaker, B. R. (2009). Storage retrogradation behavior of sorghum, maize and rice starch pastes related to amylopectin fine structure. *Journal of Cereal Science*, *50*, 74–81.

Miles, M., Morris, V., Orford, P., & Ring, S. (1985). The roles of amylose and amylopectin in the gelation and retrogradation of starch. *Carbohydrate Research*, *135*, 271–281.

Nishiyama, Y., Mazeau, K., Morin, M., Cardoso, M. B., Chanzy, H., & Putaux, J.-L. (2010). Molecular and crystal structure of 7-fold V-amylose complexed with 2-propanol. *Macromolecules*, *43*, 8628–8636.

Parker, R., & Ring, S. G. (2001). Mini review. Aspects of the physical chemistry of starch. *Journal of Cereal Science*, *34*, 1–17.

Pérez, S., & Bertoft, E. (2010). The molecular structures of starch components and their contribution to the architecture of starch granules: A comprehensive review. *Starch/Stärke*, *62*, 389–420.

Pushpadass, H. A., Kumar, A., Jackson, D. S., Wehling, R. L., Dumais, J. J., & Hanna, M. A. (2009). Macromolecular changes in extruded starch-films plasticized with glycerol, water and stearic acid. *Starch/Stärke*, *61*, 256–266.

Qiao, X., Tang, Z., & Sun, K. (2011). Plasticization of corn starch by polyol mixtures. *Carbohydrate Polymers*, *83*, 659–664.

Radley, J. A. (1976). *Industrial uses of starch and its derivatives*. London: Applied Science Publishers Ltd., p. 276, ISBN-10: 0853346623.

Raquez, J. M., Nabar, Y., Srinivasan, M., Shin, B. Y., Narayan, R., & Dubois, P. (2008). Maleated thermoplastic starch by reactive extrusion. *Carbohydrate Polymers*, *74*, 159–169.

Sánchez, T., & Aristizábal, J. (2007). *Guía técnica para producción y análisis de almidón de yuca*. Boletín de servicios agrícolas de la FAO., p. 163, ISSN 1020-4334.

Shi, Y. C., & Seib, P. A. (1995). Fine structure of maize starches from four *wx*-containing genotypes of the W64A inbred line in relation to gelatinization and retrogradation. *Carbohydrate Polymers*, *26*, 141–174.

Shogren, R. L., Fanta, G. F., & Felker, F. C. (2006). X-ray diffraction study of crystal transformations in spherulitic amylose/lipid complexes from jet-cooked starch. *Carbohydrate Polymers*, *64*, 444–451.

Singh, N., Singh, J., Kaur, L., Singh Sodhi, N., & Singh Gill, B. (2003). Morphological, thermal and rheological properties of starches from different botanical sources. *Food Chemistry*, *81*, 219–231.

Srichuwong, S., Sunarti, T., Mishima, T., Isono, N., & Hisamatsu, M. (2005). Starches from different botanical sources I: Contribution of amylopectin fine structure to thermal properties and enzyme digestibility. *Carbohydrate Polymers*, *60*, 529–538.

Taguet, A., Huneault, M., & Favis, B. (2009). Interface/morphology relationships in polymer blends with thermoplastics starch. *Polymer*, *50*, 5733–5743.

Takizawa, F. F., Da Silva, G. O., Konkel, F. E., & Demiate, I. M. (2004). Characterization of tropical starches modified with potassium permanganate and lactic acid. *Brazilian Archives of Biology and Technology*, *47*, 921–931.

Tan, I., Wee, C. C., Sopade, P. A., & Halley, P. J. (2004). Investigation of the starch gelatinisation phenomena in water–glycerol systems: Application of modulated temperature differential scanning calorimetry. *Carbohydrate Polymers*, *58*, 191–204.

Tang, H., Watanabe, K., & Mitsunaga, T. (2002). Structure and functionality of large, medium and small granule starches in normal and waxy barley endosperms. *Carbohydrate Polymers*, *49*, 217–224.

Tester, R. F., Karkalas, J., & Qi, X. (2004). Starch composition, fine structure and architecture. *Journal of Cereal Science*, *39*, 151–165.

Tharanathan, R. N. (2005). Starch—Value addition by modification. *Critical Reviews in Food Science and Nutrition*, *45*, 371–384.

Thunwall, M., Boldizar, A., & Rigdahl, M. (2006). Extrusion processing of high amylose potato starch materials. *Carbohydrate Polymer*, *65*, 441–446.

Thys, R. C. S., Westfahl, H., Jr., Norña, C. P. Z, Marczak, L. D. F., Silveira, N. P., & Cardoso, M. B. (2008). Effect of the alkaline treatment on the ultrastructure of C-type starch granules. *Biomacromolecules*, *9*, 1894–1901.

Van Soest, J. J. G., Benes, K., & De Wit, D. (1996). The influence of starch molecular mass on the properties of extruder thermosplastic starch. *Polymer*, *37*, 3543–3552.

Van Soest, J. J. G., Hulleman, S. H. D., De Wit, D., & Vliegenthart, J. F. G. (1996). Crystallinity in starch bioplastics. *Industrial Crops and Products*, *5*(1), 1–122.

Wang, S. J., Liu, H. Y., Gao, W. Y., Chen, H., Yu, J., & Xiao, P. (2006). Characterization of new starches separated from different Chinese yam (*Dioscorea opposita* Thunb.) cultivarsv. *Food Chemistry*, *99*, 30–37.

Wang, T. L., Bogracheva, T. Y., & Hedley, C. L. (1998). Starches: As simple as A,B,C? *Journal of Experimental Botany*, *49*, 481–502.

Xia, L., Wenyuan, G., Qianqian, J., Luqi, H., & Changxiao, L. (2011). Study on the morphology, crystalline structure, and thermal properties of *Fritillaria ussuriensis* maxim starch acetates with different degrees of substitution. *Starch/Stärke*, *63*, 24–31.

Yu, L., & Christie, G. (2005). Microstructure and mechanical properties of orientated thermoplastic starches. *Journal of Materials Science*, *40*, 111–116.

Zobel, H. F. (1988). Molecules to granules—A comprehensive starch review. *Starch/Stärke*, *40*, 44–50.

Zhou, X. Z., Cui, Y. F., Jia, D. M., & Xie, D. (2009). Effect of a complex plasticizer on the structure and properties of the thermoplastic PVA/starch blends. *Polymer: Plastics Technology and Engineering*, *48*, 489–495.

Zullo, R., & Iannace, S. (2009). The effects of different starch sources and plasticizers on film blowing of thermoplastic starch: Correlation among process, elongational properties and macromolecular structure. *Carbohydrate Polymers*, *77*, 376–383.